DOI: 10.1002/ange.201308903

Single-Molecule Studies

Direct and Single-Molecule Visualization of the Solution-State Structures of G-Hairpin and G-Triplex Intermediates**

Arivazhagan Rajendran, Masayuki Endo, Kumi Hidaka, and Hiroshi Sugiyama**

Abstract: *We present the direct and single-molecule visualization of the in-pathway intermediates of the G-quadruplex folding that have been inaccessible by any experimental method employed to date. Using DNA origami as a novel tool for the structural control and high-speed atomic force microscopy (HS-AFM) for direct visualization, we captured images of the unprecedented solution-state structures of a tetramolecular antiparallel and (3+1)-type G-quadruplex intermediates, such as G-hairpin and G-triplex, with nanometer precision. No such structural information was reported previously with any direct or indirect technique, solution or solid-state, single-molecule or bulk studies, and at any resolution. Based on our results, we proposed a folding mechanism of these G-quadruplexes.*

Guanidine-rich sequences are abundant in human chromosomal telomere DNA and are found as a single-stranded TTAGGG tandem repeats at 3′-overhangs.[1] They have also been identified in other regions, such as promoter regions of several proto-oncogenes including *c-myc*, *c-kit*, and *K-ras*.[2] These sequences are predicted to form non-canonical G-quadruplex structures. It has been estimated that more than 376000 G-quadruplexes are present in the human genome.[2,3] These sequences are also found in several other organisms.[4] The G-quadruplex has become an exciting therapeutic target since it was initially identified. For instance, developing a drug that can competitively bind and replace shelterin (a nucleoprotein complex that shapes, covers, and protects the G-rich telomere ends from the DNA-damage-response machinery) from telomere ends can possibly lead to cell death.[5] Quadruplex structures are expected to play a major role in various cellular processes, such as chromosomal alignment, replication, transcription, genome recombination, and to exert control over cancer-cell proliferation.[2,6,7] The identification of G-quadruplex-stabilizing[8,9] and destabilizing[10,11] proteins further supported the assumption that these structures have potential significance in various biological processes. Moreover, G-rich sequences have been shown to inhibit HIV type-1 replication in culture.[12]

Besides the investigations of the biological significance of G-quadruplexes and therapeutic interests for cancer and AIDS, the studies on the folding pathway of G-quadruplexes and the intermediate states involved are of ongoing interest. Only a few studies have been carried out on the folding pathway of quadruplexes and most of them were either based on theoretical calculations[13–15] or assumptions derived from the experimental evidence.[16–23] To date, very little is known on the intermediates and this is mainly due to the lack of techniques that can successfully isolate the intermediates. Based on the computational studies, we have recently proposed a folding pathway for the human telomeric G-quadruplexes (Figure 1 a) that progresses through intermediate states, such as G-hairpin (a G–G mismatched Hoogsteen duplex formed by two tandem guanine repeats) and G-triplex (a partly folded structure with three tandem guanine repeats bound together by Hoogsteen hydrogen bonding). Spectroscopic techniques, such as UV/Vis,[19] circular dichroism (CD),[16–18] fluorescence resonance energy transfer (FRET)[18] and NMR,[21] calorimetric studies, such as differential scanning calorimetry (DSC) and isothermal titration calorimetry (ITC),[17] kinetic methods, such as stopped-flow,[19] force-based methods, such as optical[16] and magnetic[20] tweezers, and a protein ion channel[22] have been applied to investigate the intermediate states in the quadruplex folding. All these studies derived only indications for the presence of intermediates and speculated that the intermediate is a G-triplex. Further, almost no evidence is derived for the involvement of G-hairpins in the folding process. Thus, it is not clear whether the folding process involves two steps with three monomolecular conformations (unfolded, triplex, and quadruplex) or three steps with four monomolecular conformations (unfolded, hairpin, triplex, and quadruplex). Therefore, for the precise determination of intermediates, direct visualization of the solution-state structure of the intermediates involved in the folding process of G-quadruplex is highly desired.

[*] Dr. A. Rajendran,[+] K. Hidaka, Prof. Dr. H. Sugiyama
Department of Chemistry, Graduate School of Science
Kyoto University
Kitashirakawa-oiwakecho, Sakyo-ku, Kyoto 606-8502 (Japan)
E-mail: hs@kuchem.kyoto-u.ac.jp
Prof. Dr. M. Endo, Prof. Dr. H. Sugiyama
Institute for Integrated Cell-Material Sciences (WPI-iCeMS)
Kyoto University
Yoshida-ushinomiyacho, Sakyo-ku, Kyoto 606-8501 (Japan)
and
CREST, Japan Science and Technology Corporation (JST)
Sanbancho, Chiyoda-ku, Tokyo 102-0075 (Japan)
E-mail: endo@kuchem.kyoto-u.ac.jp
[+] Current address: Faculty of Medicine and Life Science Center of TARA, University of Tsukuba
1-1-1 Tennodai, Tsukuba-shi, Ibaraki-ken 305-8577 (Japan)

[**] This work was supported by Core Research for Evolutional Science and Technology (CREST) of JST and JSPS KAKENHI (Grant Numbers 24310097, 24225005, 24104002). Financial support from The Mitsubishi Foundation and The Asahi Glass Foundation to M.E. are also acknowledged. A.R. expresses sincere thanks to JSPS for the Postdoctoral fellowship.

Supporting information for this article is available on the WWW under http://dx.doi.org/10.1002/anie.201308903.

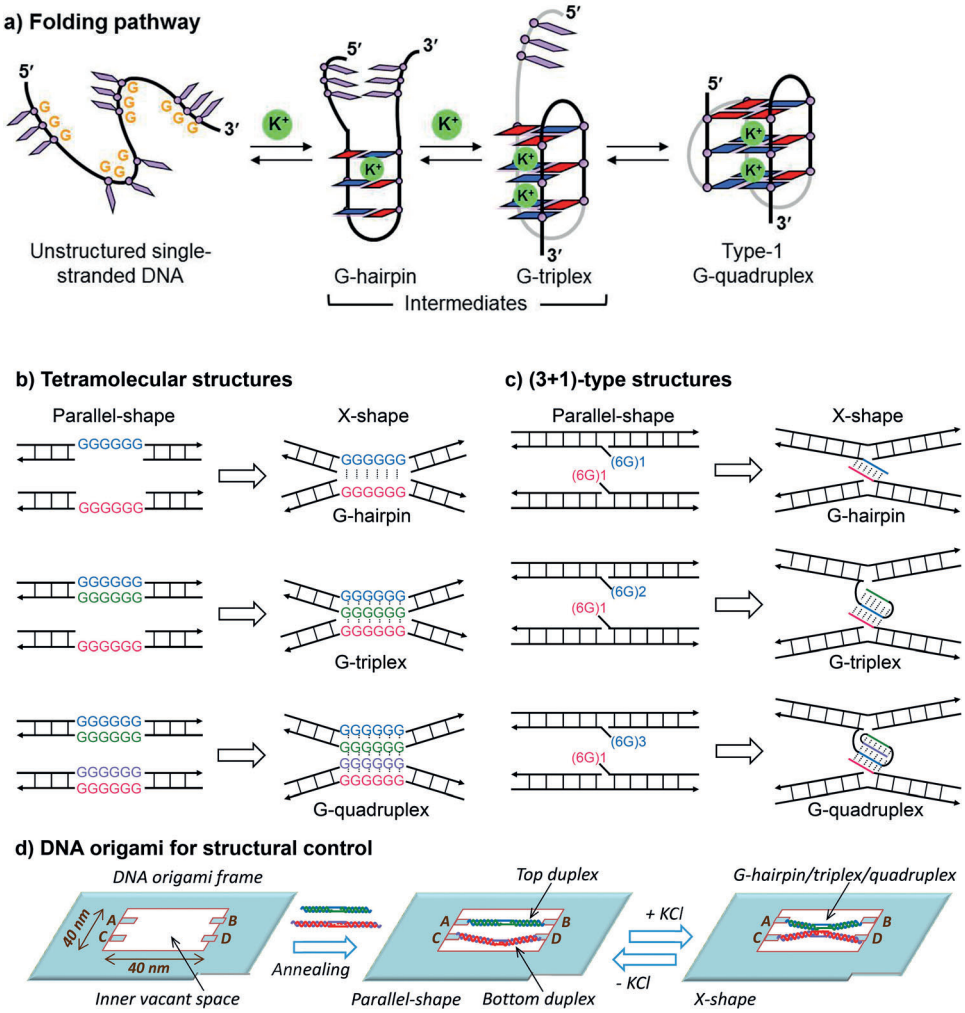

Figure 1. a) Proposed folding pathway of human telomeric type-1 G-quadruplex. Schematic representation of b) a tetramolecular c) and (3+1)-type G-hairpin, G-triplex and G-quadruplexes. 6G represents the sequence GGGGGGTTN, where N = A or T. For (3+1)-type, we have also tested three G-repeats. The arrow head in the DNA sequences indicates the 3′ end. d) Schematic representation of the DNA origami frame with G-repeats containing duplexes and KCl-promoted conformational changes in the incorporated duplexes.

Herein we utilize a DNA origami frame[24–28] to structurally and stoichiometrically control the DNA sequences (see Supporting Information, Figure S1) so that a particular intermediate can be selectively formed, and used high-speed atomic force microscopy (HS-AFM)[29–34] to directly visualize the intermediates. For this investigation, we have adopted two types of structures: 1) a tetramolecular antiparallel;[28] and 2) (3+1)-type[27] G-quadruplex structures. The formation of a particular structure is achieved by controlling the incorporated strands that contain contiguous G residues in case of tetramolecular structures, and the number of G-repeats in case of (3+1)-type structures. For the tetramolecular G-hairpin-forming sequences, we adopted two unique Watson–Crick duplexes each contained six contiguous G residues opposite to a nick in the complementary strand (see, Figure 1 b, G-hairpin and Supporting Information Figure S2). In this way, we could incorporate only two G-repeat strands out of the four participating strands, and aim to form the G-hairpin structure specifically. In case of tetramolecular G-triplex, the top duplex had six G–G mismatches in the middle, while the bottom duplex contained six contiguous G residues opposite a nick in the complementary strand (Figure 1 b, G-triplex and Supporting Information, Figure S2). This will leave only three strands with G-repeat sequences in the middle which in turn can lead to the formation of G-triplex structure specifically. We have recently investigated on the KCl-induced tetramolecular antiparallel G-quadruplex formation in which both the duplexes contained six G–G mismatches in the middle (Figure 1 b, G-quadruplex and Supporting Information, Figure S1–S2).[28] For comparison, we adopted those data herein. To bring the duplexes closer, particularly the G–G-mismatch regions, and to promote the formation of desired intermediates, we imposed structural flexibility in the strands by increasing their length. As a result, the length of the top and bottom duplexes used were 67 and 77 base pairs (bp) respectively, while the length between two connecting sites in origami frame was 64 bp.

To achieve the (3+1)-type G-hairpin, we have used two duplexes each containing a single-stranded overhang with GGGGGGTTN (where N = A or T) sequence (Figure 1 c, G-hairpin and Figure S3). The top duplex had two repeats of the GGGGGGTTN ((6G)2 where N = A or T) sequence while the bottom duplex contained one such sequence in case of (3+1)-type G-triplex (Figure 1 c, G-triplex and Figure S3). For the G-quadruplex, we have used three such repeats in the top duplex while one such sequence in the bottom duplex (Figure 1 c, G-quadruplex and Figure S3). We have also studied (3+1)-type structures that contained three contiguous G residues as it is naturally abundant (Figure S4). All the duplex DNAs used herein contained single-stranded regions each 16 bases in length at both the termini that are needed for their attachment inside the origami frame through complementary base pairing. The conformational switching was observed using HS-AFM by monitoring the topological changes of the duplexes from parallel to X-shape. Note, the G-hairpins we have prepared were basically G–G duplexes.

These structures are analogous to the intramolecular hairpin and thus termed G-hairpin throughout.

In each case the origami frame with incorporated duplexes was prepared, purified, immobilized on a mica surface and imaged by AFM. The absence of any significant structural formation will result in no interaction between the duplexes at contiguous G residues. This in turn can be visualized as a parallel-shape of the duplexes in the AFM image. The formation of a notable structure will bring the duplexes closer in the middle and can be seen as X-shape (Figure 1 d). We first characterized the topology of the tetramolecular hairpin and triplex forming sequences in 20 mM Tris-HCl buffer containing 5 mM $MgCl_2$. As can be seen from the representative image given in Figure 2 left, part (a), in most cases (73%) the incorporated duplexes for the hairpin system lay parallel to each other. A similar trend was obsereved the triplex in which 76% of the duplexes adopted the parallel-shape (Figure 2 left, part (c)). This clearly indicated that at low ionic strength, the formation of hairpin and triplex intermediates are less pronounced. However, a minor but significant amount of such intermediates were formed even in the presence of only 5 mM Mg^{2+} (data not shown). Next, the analysis was performed by the concurrent addition of 10 mM $MgCl_2$ and 100 mM KCl. Surprisingly, the duplexes adopted X-shape in both the cases with relatively higher yield of 62 and 57% for hairpin (Figure 2 left, part (b)) and triplex (Figure 2, left, part (d), also Figure S5), respectively. This X-shape was always observed in the middle of the incorporated strands where the contiguous G residues were present, and no interaction was found on other regions, indicating the formation of intermediate structures and not simple overlap of the duplexes. A similar trend was obtained for (3+1)-type hairpin and triplex sequences with either six (Figure 2, middle, and Figure S6) or three (Figure 2, right, also Figure S7) contiguous G residues. In the absence of KCl, most of the duplexes had a parallel-shape for both hairpin and triplex sequences, while the addition of KCl induced the formation of the X-shape. In this case, notable structures were observed in between the duplexes where the single-stranded overhangs were placed.

Having directly visualized the intermediates, we then estimated the quantitative yields of G-hairpin and G-triplex intermediates in each case as summarized in Table 1. As described above, at low ionic strength (5 mM Mg^{2+}), only a small amount of X-shapes were obtained for the tetramo-

Table 1: The yield [%] of X-shapes calculated for the G-repeats containing samples.

Sequences	Tetramolecular structures								
	G-hairpin			G-triplex			G-quadruplex		
	5 mM Mg^{2+}	10 mM Mg^{2+}	10 mM Mg^{2+} and 100 mM K^+	5 mM Mg^{2+}	10 mM Mg^{2+}	10 mM Mg^{2+} and 100 mM K^+	5 mM Mg^{2+}	10 mM Mg^{2+}	10 mM Mg^{2+} and 100 mM K^+
6 G-G/G-G	27 (416)	64 (295)	62 (191)	24 (153)	32 (114)	57 (182)	18 (331)[a]	23 (374)[a]	76 (276)[a]
	(3+1)-Type structures								
6 G-G-G/G	24 (532)	23 (313)	37 (263)	29 (346)	43 (291)	54 (121)	26 (406)	32 (277)	69 (199)
3 G-G-G/G	6 (345)	12 (188)	10 (187)	11 (432)	15 (226)	17 (219)	16 (331)	20 (272)	44 (244)[b]

[a,b] Data taken from our parallel studies, references [28] and [27] respectively. Numbers in the parenthesis indicate the number of origami tiles counted in each case. [Tris-HCl] = 20 mM, pH 7.6; [$MgCl_2$] = 5 or 10 mM; [KCl] = 0 or 100 mM.

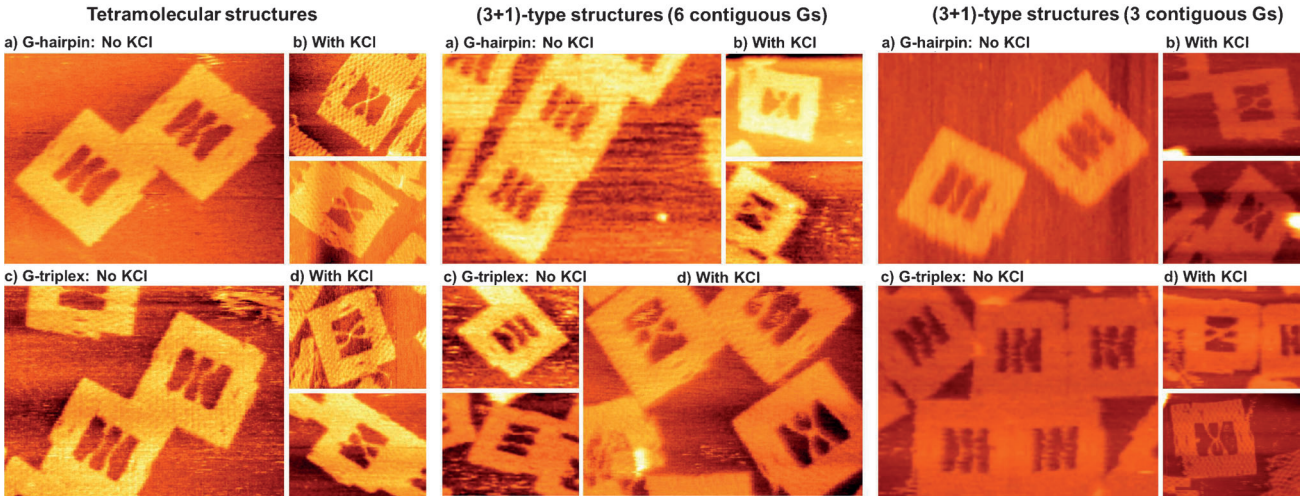

Figure 2. AFM images of the DNA origami frame with incorporated duplexes for the tetramolecular antiparallel structures (left) and (3+1)-type structures with six (middle) and three (right) contiguous G residues. Top panels: G-hairpin structures recorded in the absence (a) and presence (b) of KCl. Bottom panels: G-triplex structures recorded in the absence (c) and presence (d) of KCl. [Tris-HCl] = 20 mM, pH 7.6; [$MgCl_2$] = 5 mM (a and c) or 10 mM (b and d); [KCl] = 0 mM (a and c) or 100 mM (b and d). Image size: 300×225 nm (large images) and 200×150 nm (small images).

lecular G-hairpin, G-triplex, and G-quadruplex. The yield increased for all three structures at higher ionic strength (either 10 mM Mg^{2+} alone or simultaneous presence of 10 mM Mg^{2+} and 100 mM K^+). Interestingly, the maximum yield for the tetramolecular G-hairpin (64%) was obtained in the presence of 10 mM Mg^{2+} alone and additional 100 mM K^+ did not cause any increase in the yield, rather a slight decrease (62%) was observed. However, maximum X-shapes were obtained in the presence of concurrent addition of 10 mM Mg^{2+} and 100 mM K^+ for triplex (57%) and quadruplex (76%). The trends in yield in the presence of different concentrations follow the order, in 5 mM Mg^{2+}: hairpin > triplex > quadruplex; in 10 mM Mg^{2+}: hairpin > triplex > quadruplex; in 10 mM Mg^{2+} and 100 mM K^+: quadruplex > hairpin ≈ triplex. From these trends, we could interpret that the G-hairpin selectively prefers Mg^{2+} over K^+ ions, or in other words, formation of G-hairpin is preferentially promoted by Mg^{2+}. As it is well established, the formation of the G-quadruplex is induced by K^+. Our yield calculations further indicated that the G-triplex prefers neither Mg^{2+} nor K^+, while it seems to prefer both the ions moderately.

Note, our ab initio and fragment molecular orbital calculations[14] indicated that the G-triplex structure contains only one channel K^+-binding site when the calculations were carried out exclusively in the presence of K^+ ions. By considering present observations and previous results,[14] we may hypothesize that in the simultaneous presence of K^+ and Mg^{2+}, the second site could be occupied by Mg^{2+} as the G-triplex has moderate preference for both these ions. From these interpretations, we could conclude that there may be interplay between the divalent Mg^{2+} and monovalent K^+ ions when the unstructured G-rich sequence folds into a G-quadruplex structure through hairpin and triplex intermediates. Further, the initial folding (such as hairpin and triplex) may be better initiated or stabilized if Mg^{2+} is present. Note, Mg^{2+} and K^+ are the most abundant divalent and monovalent cations, respectively, in the cytoplasm of a cell. Thus, this interplay is biologically significant. A similar conformational transition by the interplay of Mg^{2+} and K^+ was recently reported for the Watson–Crick hairpin and Hoogsteen G-quadruplex.[35] Herein we report that such mono- and divalent-cation-mediated interplay also takes place between Hoogsteen G-hairpin and G-quadruplex structures. A comparable trend was also obtained for (3+1)-type structures with slight deviations. The good yield of the intermediates in each case indicates that these are not short-living species, but rather stable intermediates.

We have also tested the topography of the control sequences that were prepared by introducing the G–T and T–T mismatches by mutating G into T (Figure S8–S9). The yield analysis was performed in selective cases as listed in Table S1 in the Supporting Information. In all the cases tested, we could find only 2 to 3% of X-shapes, indicating that these strands are not capable of forming a notable structure. This result further indicated that the formed X-shapes in case of G-rich strands are due to the formation of characteristic structures and not simple overlap of the incorporated duplexes.

Our recent report of the ab initio calculations on the stabilization energies of different base pairs indicated that Hoogsteen G–G base pair (-18.4 kcal mol^{-1}) is as stable as a Watson–Crick A–T base pair (-19.0 kcal mol^{-1}).[14] It further indicated that the stability of different Hoogsteen base pairs follows the order: G–G base pair (-9.2 kcal mol^{-1} per guanine) < G-triplet (-16.9 kcal mol^{-1} per guanine) ≈ G-tetrad (-17 kcal mol^{-1} per guanine). Having observed the negative stabilization energies, all three Hoogsteen structures are feasible. The G-hairpin structure may have stability similar to that of the A–T duplex. The G-triplex is energetically similar to the G-quadruplex. Note, these calculations were carried out without considering the base stacking and effect of cations. If we consider both of these effects, then we may assume that the quadruplex may have slightly better stabilization energy than the triplex as the G-tetrad could have better stacking than a G-triplet. Our experimental yields from the presence of both 10 mM Mg^{2+} and 100 mM K^+, follow the trends observed in the energy calculations. For instance, the yield of (3+1)-type structures with six contiguous Gs follow the order: G-hairpin (37%) < G-triplex (54%) < G-quadruplex (69%). Same trend was also observed for the sequences that contained three contiguous Gs: G-hairpin (10%) < G-triplex (17%) < G-quadruplex (44%). The better stabilization energy leads to an increased yield of a particular structure over the other. The tetramolecular antiparallel structure slightly deviates from this as the observed trend follows the order: G-triplex (57%) ≈ G-hairpin (62%) < G-quadruplex (76%). However, only a small difference in the yield of G-triplex and G-hairpin is observed. This may be partly due to the interplay between the divalent Mg^{2+} and monovalent K^+ as explained above.

The reasons for the inability of the bulk experimental techniques to produce detectable signal for the formation of G-hairpin could be: 1) As our theoretical calculations indicated,[14] the hairpin structure is a higher energy conformation than that of the triplex and quadruplex. Thus the formed hairpin might rapidly convert into a triplex. 2) The G-hairpin structure has a greater preference for the divalent Mg^{2+} and thus experiments may have to be carried out in the presence of Mg^{2+}, possibly using double-mixing stopped-flow techniques to investigate the complete folding mechanism. 3) The recent stopped-flow investigation on quadruplex folding by Zhang and Balasubramanian elucidated that the folding process involves two kinetic steps with at least one intermediate.[19] The first kinetic step is the formation of the triplex and the second step is the final folding into a quadruplex structure. The first step follows the faster kinetics which is speculated to include the cation (K^+) binding pre-equilibrium step, hairpin and triplex formations. While the second step is slower than the first step and it was assumed to involve the second K^+ binding and the final folding of quadruplex structure. Owing to the fast kinetics of the triplex formation, it is difficult to follow the formation of hairpin and its kinetics even using the stopped-flow method,[19] and also due to the small population of the hairpin structure it is even difficult to study using optical methods.[16–19] The reason that we could observe the hairpin structure with surprisingly high yield could be due to the lack of third and fourth strands that

contain G-repeats in the case of the tetramolecular structure, and third and fourth tandem G-repeats for the (3+1)-type structures. This possibly led to the initial folding and locked into the G-hairpin conformation as no further folding is possible. This in turn might have increased the yield of the hairpins. This situation is the same for the triplex structures which have a considerably larger population.

The role of HS-AFM in elucidating the folding pathway of a tetramolecular antiparallel and (3+1)-type G-quadruplexes are summarized in Figure 3. The unstructured single-stranded G-rich sequence may initially fold into a G-hairpin which is stabilized preferentially by Mg^{2+} ions. This initially folded structure is sufficiently stable and may be in equilibrium with the unstructured single-stranded DNA. The stability of this structure might dependent on the concentration of the mono or divalent cations. Further folding of the initially folded G-hairpin could result in the G-triplex which seems to have a moderate preference for both Mg^{2+} and K^+ ions. Final folding results in the formation of the G-quadruplex structure which is promoted by K^+ ions. The preference of Mg^{2+} ions for the formation of the G-hairpin is reasonable, because it was reported[36] that the thermodynamic stability of RNA hairpin structures is dependent on the concentration of divalent cations, especially Mg^{2+}. Such a cation dependent conformational transition between a quadruplex and Watson–Crick hairpin was also reported for DNA sequences.[37] However, for the G-quadruplex, the perfect size matching of the K^+ ion would make it fit exactly to the G-tetrad core. Besides, our data alone is not sufficient to derive the role of mono and divalent cations and the interplay between them in the G-quadruplex folding process, and further studies are required. The present results are in good agreement with our theoretical calculations that were carried out recently on human telomeric type-1 and type-2 G-quadruplex structures.[14] Further, our conclusion, that is, the formation of the G-quadruplex proceeds in discrete steps progressing through stable intermediates, is well supported by the previous investigations.[16–19]

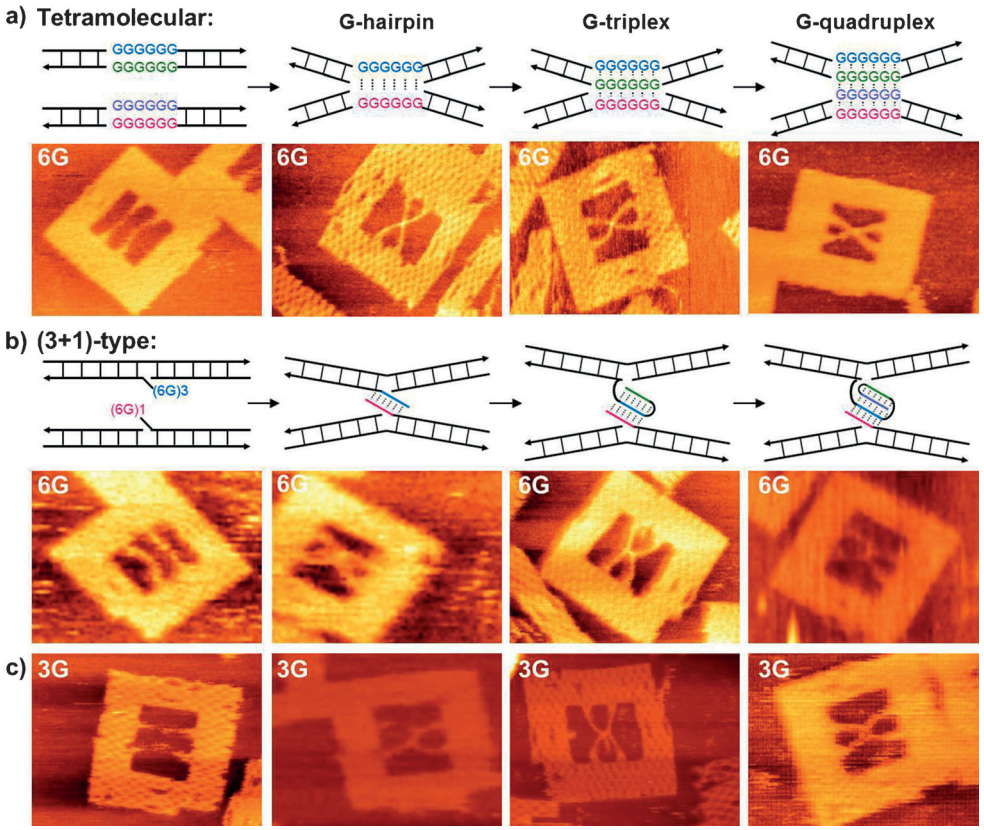

Figure 3. The folding pathways of a tetramolecular (a) and (3+1)-type (b and c) G-quadruplexes that contain six (a and b) and three (c) G-repeats. The single stranded G-repeat sequence initially forms a Hoogsteen type G-hairpin which consecutively folds into a G-triplex before the formation of the final G-quadruplex structure. The arrow head in the graphical representation of the DNA sequences indicates the 3′ end. Image size: 200×150 nm. [Tris-HCl] = 20 mM, pH 7.6; [$MgCl_2$] = 5 mM (parallel-shapes) or 10 mM (X-shapes); [KCl] = 0 mM (parallel-shapes) or 100 mM (X-shapes).

Although the folding pathway described in Figure 3 proceeds through stepwise strand addition, we cannot ignore two other possibilities: 1) the dimerization of the G-hairpin to form the G-quadruplex; and 2) G-triplex–G-triplex disproportion to yield a G-quadruplex and a G-hairpin. By considering the presence of G-hairpin, all three folding pathways are possible. However, the stepwise formation and triplex–triplex disproportionation must proceed through a stable G-triplex intermediate. Also, the formation of a quadruplex may involve the combination of all these folding pathways rather than a single folding mechanism.

In addition, we have no information about the slipped-strand conformations reported previously[13] in which not all the guanines base pair as in the case of the native G-quadruplex. Previous stabilization energy calculations[14] indicated that the higher the number of Hoogsteen base pairs, the greater the stability of the structure. Also, it is anticipated that all-guanine base pairing as in the native G-quadruplex structure may give better stacking. Based on this, we assume that the base-pairing patterns in both the intermediates should be as observed in the native quadruplex. Our assumption is also supported by the recent NMR spectroscopy study[21] which indicated the formation of a G-triplex with Hoogsteen-like hydrogen bonding as observed in the quadruplex structure.

In conclusion, we present herein the direct visualization of the solution-state structures of the in-pathway intermediates of the G-quadruplex folding that have been inaccessible by any other experimental method. Using DNA origami as a tool to control the strand polarity, stoichiometry and number of G-repeats or G-repeat containing strands, we captured the images of the unprecedented solution-state structures of a tetramolecular antiparallel and (3+1)-type G-quadruplex intermediates such as G-hairpin and G-triplex with nanometer precision. No structural information on these intermediates was reported previously with any direct or indirect techniques, solution or solid-state, single-molecule or bulk studies and at any resolution. Further, our investigations indicated that they are stable intermediates and formed with good yield. The interplay between the divalent Mg^{2+} and monovalent K^+ ions during the quadruplex folding process through hairpin and triplex intermediates was elucidated. Our HS-AFM analysis provided novel information that helped us to update the folding model of the G-quadruplex structures. We anticipate that this pioneering structural investigation at the single-molecule level will be helpful to understand the folding of various other G-quadruplex structures which in turn will be beneficial for the development of drugs targeting G-quadruplex structures. Preliminary investigations on the G-quadruplex-binding ligand and proteins indicate that they are also capable of binding and inducing the G-hairpin and G-triplex intermediates, evidencing the biological and therapeutic importance of these intermediates. These results will be presented elsewhere.

Received: October 12, 2013
Revised: December 17, 2013
Published online: March 12, 2014

Keywords: atomic force microscopy · DNA origami · G-hairpin · G-quadruplex · G-triplex

[1] V. L. Makarov, Y. Hirose, J. P. Langmore, *Cell* **1997**, *88*, 657 – 666.
[2] H. Fernando, A. P. Reszka, J. Huppert, S. Ladame, S. Rankin, A. R. Venkitaraman, S. Neidle, S. Balasubramanian, *Biochemistry* **2006**, *45*, 7854 – 7860.
[3] A. T. Phan, Y. S. Modi, D. J. Patel, *J. Am. Chem. Soc.* **2004**, *126*, 8710 – 8716.
[4] P. Sarkies, C. Reams, L. J. Simpson, J. E. Sale, *Mol. Cell* **2010**, *40*, 703 – 713.
[5] T. de Lange, *Genes Dev.* **2005**, *19*, 2100 – 2110.
[6] A. Rizzo, E. Salvati, M. Porru, C. D'Angelo, M. F. Stevens, M. D'Incalci, C. Leonetti, E. Gilson, G. Zupi, A. Biroccio, *Nucleic Acids Res.* **2009**, *37*, 5353 – 5364.
[7] K. Muniyappa, *Med. Chem. Res.* **2010**, *19*, S28 – S29.
[8] G. Fang, T. R. Cech, *Cell* **1993**, *74*, 875 – 885.
[9] L. Uliel, P. Weisman-Shomer, H. Oren-Jazan, T. Newcomb, L. A. Loeb, M. Fry, *J. Biol. Chem.* **2000**, *275*, 33134 – 33141.
[10] N. Baran, L. Pucshansky, Y. Marco, S. Benjamin, H. Manor, *Nucleic Acids Res.* **1997**, *25*, 297 – 303.
[11] H. Sun, J. K. Karow, I. D. Hickson, N. Maizels, *J. Biol. Chem.* **1998**, *273*, 27587 – 27592.
[12] J. A. Este, C. Cabrera, D. Schols, P. Cherepanov, A. Gutierrez, M. Witvrouw, C. Pannecougue, Z. Debyser, R. F. Rando, B. Clotet, J. Desmyter, E. D. Clercg, *Mol. Pharmacol.* **1998**, *53*, 340 – 345.
[13] R. Štefl, T. E. Cheatham III, N. Špačková, E. Fadrná, I. Berger, J. Koča, J. Šponer, *Biophys. J.* **2003**, *85*, 1787 – 1804.
[14] T. Mashimo, H. Yagi, Y. Sannohe, A. Rajendran, H. Sugiyama, *J. Am. Chem. Soc.* **2010**, *132*, 14910 – 14918.
[15] P. Stadlbauer, M. Krepl, T. E. Cheatham III, J. Koca, J. Sponer, *Nucleic Acids Res.* **2013**, *41*, 7128 – 7143.
[16] D. Koirala, T. Mashimo, Y. Sannohe, Z. Yu, H. Mao, H. Sugiyama, *Chem. Commun.* **2012**, *48*, 2006 – 2008.
[17] M. Bončina, J. Lah, I. Prislan, G. Vesnaver, *J. Am. Chem. Soc.* **2012**, *134*, 9657 – 9663.
[18] R. D. Gray, R. Buscaglia, J. B. Chaires, *J. Am. Chem. Soc.* **2012**, *134*, 16834 – 16844.
[19] A. Y. Q. Zhang, S. Balasubramanian, *J. Am. Chem. Soc.* **2012**, *134*, 19297 – 19308.
[20] W. Li, X.-M. Hou, P.-Y. Wang, X.-G. Xi, M. Li, *J. Am. Chem. Soc.* **2013**, *135*, 6423 – 6426.
[21] V. Limongelli, S. D. Tito, L. Cerofolini, M. Fragai, B. Pagano, R. Trotta, S. Cosconati, L. Marinelli, E. Novellino, I. Bertini, A. Randazzo, C. Luchinat, M. Parrinello, *Angew. Chem.* **2013**, *125*, 2325 – 2329; *Angew. Chem. Int. Ed.* **2013**, *52*, 2269 – 2273.
[22] N. An, A. M. Fleming, C. J. Burrows, *J. Am. Chem. Soc.* **2013**, *135*, 8562 – 8570.
[23] P. M. Yangyuoru, A. Y. Q. Zhang, Z. Shi, D. Koirala, S. Balasubramanian, H. Mao, *ChemBioChem* **2013**, *14*, 1931 – 1935.
[24] P. W. K. Rothemund, *Nature* **2006**, *440*, 297 – 302.
[25] M. Endo, Y. Katsuda, K. Hidaka, H. Sugiyama, *J. Am. Chem. Soc.* **2010**, *132*, 1592 – 1597.
[26] M. Endo, Y. Katsuda, K. Hidaka, H. Sugiyama, *Angew. Chem.* **2010**, *122*, 9602 – 9606; *Angew. Chem. Int. Ed.* **2010**, *49*, 9412 – 9416.
[27] Y. Sannohe, M. Endo, Y. Katsuda, K. Hidaka, H. Sugiyama, *J. Am. Chem. Soc.* **2010**, *132*, 16311 – 16313.
[28] A. Rajendran, M. Endo, K. Hidaka, P. L. T. Tran, J.-L. Mergny, H. Sugiyama, *Nucleic Acids Res.* **2013**, *41*, 8738 – 8747.
[29] A. Rajendran, M. Endo, H. Sugiyama, *Adv. Protein Chem. Struct. Biol.* **2012**, *87*, 5 – 55.
[30] A. Rajendran, M. Endo, K. Hidaka, H. Sugiyama, *J. Am. Chem. Soc.* **2013**, *135*, 1117 – 1123.
[31] A. Rajendran, M. Endo, H. Sugiyama, *Chem. Rev.* **2014**, *114*, 1493 – 1520.
[32] A. Rajendran, M. Endo, Y. Katsuda, K. Hidaka, H. Sugiyama, *ACS Nano* **2011**, *5*, 665 – 671.
[33] A. Rajendran, M. Endo, H. Sugiyama, *Angew. Chem.* **2012**, *124*, 898 – 915; *Angew. Chem. Int. Ed.* **2012**, *51*, 874 – 890.
[34] A. Rajendran, M. Endo, K. Hidaka, P. L. T. Tran, J.-L. Mergny, R. J. Gorelick, H. Sugiyama, *J. Am. Chem. Soc.* **2013**, *135*, 18575 – 18585.
[35] A. Bugaut, P. Murat, S. Balasubramanian, *J. Am. Chem. Soc.* **2012**, *134*, 19953 – 19956.
[36] A. Payle, *J. Biol. Inorg. Chem.* **2002**, *7*, 679 – 690.
[37] C. C. Hardin, T. Watson, M. Corregan, C. Bailey, *Biochemistry* **1992**, *31*, 833 – 841.

